Coulomb excitation of ^{156}Gd

M. Sugawara,[1,*] H. Kusakari,[2] Y. Yoshizawa,[3] H. Inoue,[3] T. Morikawa,[4] T. Shizuma,[5] and J. Srebrny[6]

[1]*Chiba Institute of Technology, Narashino, Chiba 275-0023, Japan*
[2]*Faculty of Education, Chiba University, Chiba 263-8522, Japan*
[3]*Faculty of Science, Hiroshima University, Higashi-hiroshima 739-8526, Japan*
[4]*Department of Physics, Kyushu University, Fukuoka 812-8581, Japan*
[5]*Kansai Photon Science Institute, Japan Atomic Energy Agency, Kizu, Kyoto 619-0215, Japan*
[6]*Heavy Ion Laboratory, Warsaw University, Pasteura 5A, PL-02-093 Warsaw, Poland*

(Received 7 September 2010; published 13 June 2011)

Multiple Coulomb-excitation experiments for ^{156}Gd were made with a 118 MeV ^{32}S beam and a 225 MeV ^{58}Ni beam. The ground-state band, the β band ($K = 0^+$), another $K = 0^+$ band, and the γ band ($K = 2^+$) were observed up to the 18^+, 14^+, 8^+, and 12^+ states, respectively, while the octupole band ($K = 1^-$) was observed up to the 15^- state, through the analysis of particle-γ-γ data. Compared with the results of the in-beam γ-ray spectroscopy previously obtained, the present result suggests that a band crossing occurs in the γ band. As for the β band, the excitation energy of the 12^+ state was revised and the 14^+ state was newly observed in the present experiment. The intrinsic matrix elements entering the generalized intensity relations were obtained so as to reproduce the spin dependence of the $E2$ matrix elements extracted from the experimental results of particle-γ angular correlation for the transitions within each band and between each band and the ground-state band by the least-squares search code GOSIA. The change of characters in the β and γ bands is discussed as a possible cause for the variation of the $E2$ matrix elements in the higher-spin region. The intrinsic matrix elements were also obtained for the $E1$ and $E3$ transitions from the ground-state band to the octupole band with $K = 1^-$ through analysis by GOSIA.

DOI: 10.1103/PhysRevC.83.064308 PACS number(s): 27.70.+q, 25.70.De, 23.20.Lv, 23.20.Js

I. INTRODUCTION

It has been recognized that the shapes of nuclei in the rare-earth region change rapidly at the neutron number $N = 90$ from the spherical shape to the axially symmetric prolate shape, if they are viewed as a function of neutron number. The ratio of the first 4^+ level energy to the first 2^+ level energy, $R_{4/2}[=E(4_1^+)/E(2_1^+)]$, has been frequently used as a collective observable for describing the transitional character. In the case of even-even Gd nuclei, the ratio $R_{4/2}$ increases from the vibrational limit of 2.0 at $N = 86$ for ^{150}Gd to the rotational limit of 3.3 at $N = 94$ for ^{158}Gd. The ratio $R_{4/2}$ for ^{156}Gd is 3.24 and almost reaches the rotational limit.

In this region, two excited bands with positive parity have been well known as the β band with $K = 0^+$ and the γ band with $K = 2^+$. Although these bands in the transitional region are often called the quasi-beta band and the quasi-gamma band, the common terms of the β band and the γ band are simply used for both cases in this article. Through the Coulomb-excitation experiments with heavy ions, Yoshizawa *et al.* [1] observed the β vibrational states and the γ vibrational states in 17 even-even nuclei in the rare-earth region in the mid 1960s. Since then, the β and γ bands have been systematically observed in the even-even Gd nuclei [2]. One can recognize from those previous results that the level order of the 0_β^+ state and the 2_γ^+ state is reversed in ^{158,160}Gd compared with that in $^{150-156}$Gd. This fact suggests that ^{156}Gd is located at an important position to understand the property of the shape transition in this region. It is also important to note that another $K = 0^+$ band has been observed in addition to the β band in this region [2]. It is desirable, therefore, to elucidate the character of the $K = 0_2^+$ band.

It is also well known that the Gd nuclei in this region are rather soft for the octupole vibrational mode. Theoretically, four octupole bands with $K = 0^-$, 1^-, 2^-, and 3^- are expected to exist in deformed nuclei. There has been, however, no example with these full members of octupole bands observed so far. It is interesting to attempt to observe a complete set of octupole bands.

It is well accepted that the unified model by Bohr and Mottelson is useful to understand the rotation-vibration structures mentioned above. The generalized intensity relation (GIR) [3], which is obtained by taking the matrix element of the transition operator in the laboratory frame with respect to the unified model wave functions, is good as a starting point to study electromagnetic transitions within bands and between bands. The intrinsic matrix elements entering the GIR can be considered as a kind of parameter from the experimental point of view, while Shimizu and Nakatsukasa [4] proposed a systematic method to calculate the intrinsic matrix elements using the microscopic cranking formalism.

In the late 1980s, Nordic groups, a Japanese group, and others started to construct a large γ-ray detector system called "NORDBALL" at the Tandem Accelerator Laboratory (TAL) at the Niels Bohr Istitute in Risø, Denmark [5]. Coulomb-excitation experiments with this modern detection system have been expected to provide valuable information on the properties of collective bands through the measurements of level energies and electromagnetic matrix elements. The

*masahiko.sugawara@it-chiba.ac.jp

purpose of this experiment is to study the level structure and the electromagnetic properties of ^{156}Gd and to characterize its collective property.

The experimental situation prior to this work is summarized as follows: Band structures were studied with in-beam γ-ray spectroscopy by using the ^{150}Nd(^{13}C, $3n\alpha$) reaction [6] and the ^{154}Sm(α, $2n$) reaction [7]. The ground-state band, the γ band, and the octupole band were observed up to 26^+, 16^+, and 21^-, respectively [6], while the β band was observed up to 10^+ [7]. The reduced transition probabilities from the ground state to the low-lying states of the β, γ, and octupole bands were extracted from the Coulomb-excitation experiment with the α beam [8]. For the higher-spin states in these bands, two experiments were performed via heavy-ion Coulomb excitation [9,10].

This article is organized as follows. First, we describe the experimental methods and results in Sec. II. Section III is allocated to discussions on the intrinsic matrix elements entering the GIR for the positive-parity bands. Brief discussions on the intrinsic matrix elements for the negative-parity bands are presented in Sec. IV. Conclusions are given in Sec. V.

II. EXPERIMENTAL METHODS AND RESULTS

Excited states of ^{156}Gd were populated through multiple Coulomb excitation with a 118 MeV ^{32}S beam and a 225 MeV ^{58}Ni beam. Experiments were made with the NORDBALL array [5,11] in the Tandem Accelerator Laboratory in Risø, Denmark. In the NORDBALL array, a Bismuth Germanium Oxide (BGO) anti-Compton spectrometer (ACS) was placed at each hexagon of a truncated icosahedron frame. As a result, a total of 20 detectors were disposed on the four rings at polar angles of 37.5°, 79.2°, 100.8°, and 142.6° with respect to the beam axis. The typical energy resolution was about 2.0 keV for 1.3 MeV γ rays. A self-supporting metallic foil of 1.0 mg/cm^2 thickness made of isotopically enriched material (93.58%) was used as a target. The beam intensity was between 10 and 20 nA during the experiment. Scattered ions were detected with five position-sensitive silicon detectors (PSDs), each of which was made of seven silicon strips as shown in Fig. 1. The detectors were placed at the backward hemisphere of the target chamber and covered the range of scattering angle $\theta_{\rm lab}$ between 103° and 154° in the laboratory system. Seven strips in each PSD were connected in series so that they could be used as a single detector. Position information was translated to ($\theta_{\rm lab}$, $\phi_{\rm lab}$) coordinates through a geometrical calculation. We used the information on the scattering angle to specify the kinematics of the scattering process for the Doppler correction of γ-ray energy as well as for the Coulomb-excitation analysis. The energy and efficiency in the NORDBALL array were calibrated with a mixed source of ^{152}Eu, ^{133}Ba, and ^{137}Cs. In addition, a ^{152}Eu source of 0.83 μCi was used to calibrate the sum-peak effects.

Experimental data were acquired in event mode when one PSD and at least one γ-ray detector were fired in coincidence. The event data were sorted offline into the particle-γ and particle-γ-γ coincidence events after the Doppler correction of γ-ray energies. The particle-γ angular correlation was extracted from the former and the E_γ-E_γ matrix was constructed from the latter. The typical energy resolution of γ-ray peaks was about 10 keV at around 1 MeV after Doppler correction. The numbers of particle-γ and particle-γ-γ coincidence events for the ^{32}S beam were 42.3×10^6 and 0.7×10^6, respectively, and those for the ^{52}Ni beam were 52.3×10^6 and 1.6×10^6, respectively.

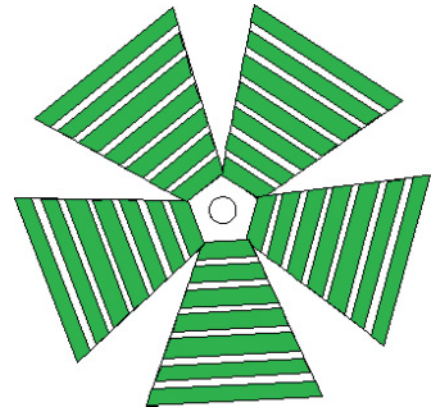

FIG. 1. (Color online) Schematic view of PSD's from downstream of the beam. Each gray strip is a position-sensitive silicon detector.

A. Results from E_γ-E_γ matrix

The E_γ-E_γ matrix was made from the ^{58}Ni-induced Coulomb-excitation data summed over the scattering angle of the particles. In spite of the poor statistics, the cleanness of the matrix enabled us to deduce the level scheme. The level scheme was constructed using the RADWARE package [13]. Our proposed level scheme is divided into three parts, each of which is shown separately in Figs. 2–4.

The ground-state band, the β band, another $K = 0^+$ band, the γ band, and an octupole band ($K = 1^-$) were observed up to 18^+, 14^+, 8^+, 12^+, and 15^-, respectively. The 12^+ and 14^+ states in the β band were observed at 2650 and 3134 keV, respectively. Since the higher spin members of the β band were well above the yrast line, they were difficult to excite by heavy-ion fusion reactions. Before this experiment, the 12^+ state had been tentatively assigned at 2708 keV [7]. Figure 5 shows an example of the gated spectra appropriate for the support on the extension of the β band. This figure shows the two pairs of $I_\beta \rightarrow I_{\rm g}$ and $I_\beta \rightarrow (I-2)_{\rm g}$ transitions from the β band to the ground-state band: one is the pair of 727 and 1235 keV transitions from the 12^+_β state and the other is the pair of 659 and 1211 keV transitions from the 14^+_β state. Excitation energies are plotted against $I(I+1)$ for the β band in Fig. 6. The 12^+ state observed in the present experiment conforms to the smooth behavior extended from the lower-spin members better than the previous experiment. The new 14^+ state shows the smooth behavior as well.

As for the γ band, we observed in-band transitions. In Fig. 7, the 432 and 513 keV transitions are shown in the coincidence spectrum obtained through the gate on the $8^+_{\rm g} \rightarrow 6^+_{\rm g}$ transition. The 513 keV transition placed on top of the 10^+_γ

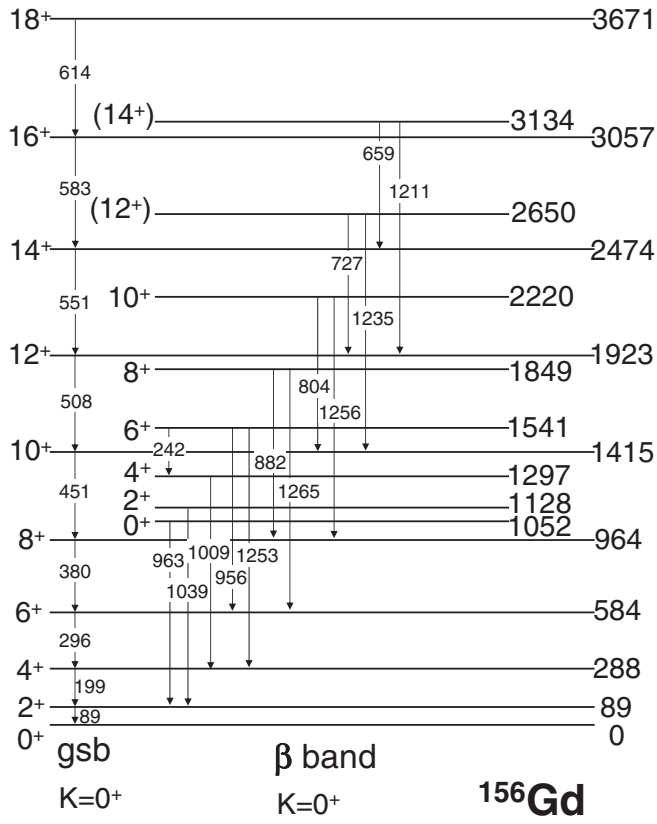

FIG. 2. Partial level scheme of ^{156}Gd proposed from the E_γ-E_γ matrix, including the ground-state band (abbreviated "gsb") and the β band. The energies of γ transitions and levels are indicated in keV.

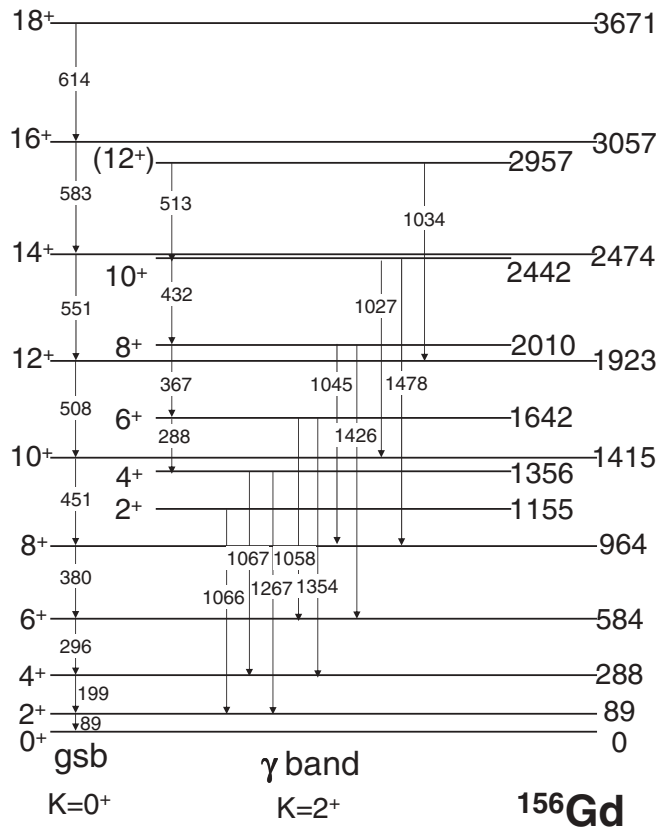

FIG. 3. Partial level scheme including the ground-state band and the γ band.

state suggests the existence of a state at 2957 keV, which is also supported by the observation of the 1034 keV transition from this state to the 12^+_g state as shown in Fig. 5. The state at 2957 keV was assigned as the 12^+_γ state based on the decay property. In the in-beam γ-ray spectroscopy [6], the 2922 keV state was assigned as the 12^+ state of the positive-parity side-band. This band had been placed on top of the known γ band and extended up to the 16^+ state. The present experiment, therefore, provides us with evidence that a band crossing occurs between the 10^+ state and the 12^+ state in the γ band.

The particle-γ-γ coincidence results also provide us with the information on the γ-ray intensities through the gated spectrum. The branching ratios of transitions from the higher-spin levels of each band were obtained from the analysis of the E_γ-E_γ matrix. These experimental results were also included in the GOSIA analysis [14,15]. The properties of the transitions from the β band to the ground-state band are summarized in Table I. The branching ratios are converted to $B(E2)$ ratios, assuming that the $I_\beta \rightarrow I_g$ transitions are pure $E2$ ones. The large reduction of $B(E2)$ ratios seen for $I_\beta \geqslant 10$ indicates that the β band changes its character between the 8^+ and 10^+ states. Theoretical values based on the Alaga rule are shown in the last two columns for comparison. It can be inferred from this comparison that a change of K value from 0 to 2 is a possible cause for the reduction of $B(E2)$ ratios. If it is the case, however, a similar reduction should be observed for the in-band transitions. This point will be discussed later. As additional information which suggests the above interpretation, the excitation energies of the β and γ bands are shown as a function of spin I in Fig. 8. The quadratic energy formulas emulating the behavior of lower-spin states are subtracted from the excitation energies to emphasize the change of behavior occurring in the higher-spin region. It is clear that a divergence from the horizontal short-dashed lines starts at around 10^+ states both in the β band and in the γ band.

B. Analysis of particle-γ angular correlation

The intrinsic matrix elements entering the GIR were obtained so as to reproduce the matrix elements extracted from the GOSIA analysis [14,15] for the experimental results of Coulomb excitation of ^{156}Gd. We constructed a γ-ray spectrum from the γ events detected by any Ge detector on one ring in coincidence with a projectile detected in a certain range of the scattering angle θ_{lab} of any PSD. The range of particles with scattering angle between 103° and 154° was divided into seven regions delimited by 110°, 117°, 125°, 133°, 141°, and 148°. In this way, we obtained a total of 28 γ-ray spectra which provided us with the particle-γ angular correlations for the individual transitions, needed as an input data set for the code GOSIA. The list in Table II shows the levels and matrix elements which were taken into account in this analysis.

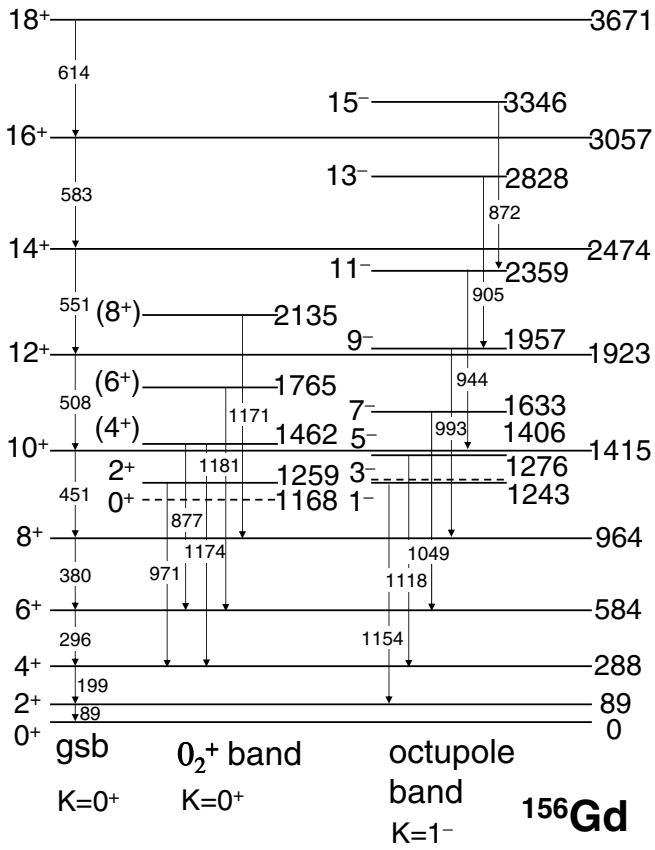

FIG. 4. Partial level scheme including the ground-state band, the 0_2^+ band, and the octupole ($K = 1^-$) band. The levels, which were not observed but have been known from the previous experiments [12], are represented by dashed lines.

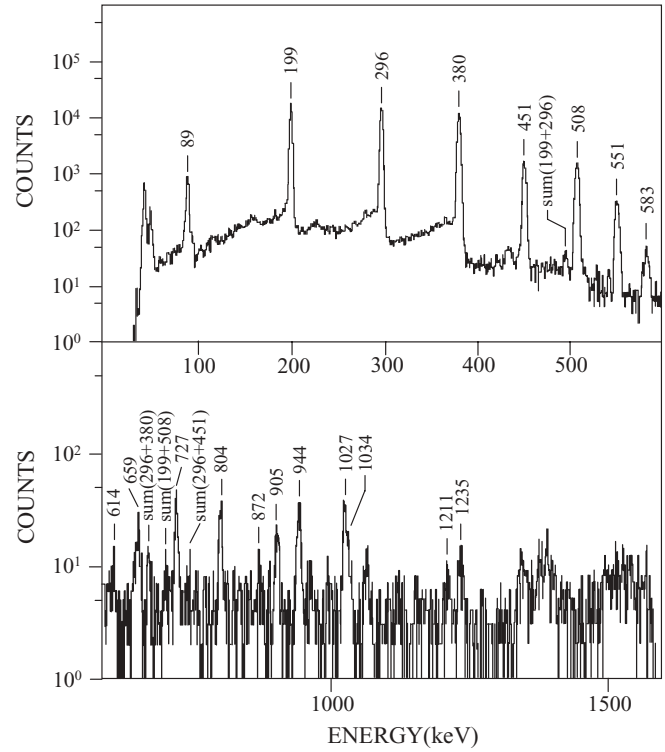

FIG. 5. γ-ray spectrum obtained by setting the gates on the 583 keV($16_g^+ \rightarrow 14_g^+$), 551 keV ($14_g^+ \rightarrow 12_g^+$), 508 keV ($12_g^+ \rightarrow 10_g^+$), and 451 keV ($10_g^+ \rightarrow 8_g^+$) transitions. Sum peaks created by the strong in-band transitions of the ground-state band are marked as, for example, "sum(296 + 380)."

The computer code GOSIA constructs the standard χ^2 function for minimization from the measured γ yields obtained in this experiment as well as the known spectroscopic data such as the lifetimes, branching ratios, mixing ratios ($E2/M1$), and the $E2$ diagonal matrix element in Table III [12]. That means $\langle 2_g^+||E2||2_g^+\rangle$ is not fixed to the value in the table but is treated rather in the same way as the measured γ yields. As mentioned in Sec. II A, we include in the GOSIA analysis the branching ratios from the higher-spin members of each band, either obtained from the analysis of the particle-γ-γ coincidence results or taken from the in-beam γ-ray spectroscopy [6], which are listed in Table IV. A total of 1478 experimental γ-ray yields were fitted by adjusting 253 matrix elements in this analysis.

The minimization process was started from the initial matrix elements, some of which were taken from the previously measured values if possible whereas others were roughly estimated on the basis of the rotational model. Since there are more than one hundred matrix elements included in this case, we cannot vary all the matrix elements simultaneously. We repeated the minimization in the following way: the matrix elements associated with the ground-state band and one of the other bands were only varied one at a time by changing the partners in turn with the ground-state band. In the course of this procedure, we took some of the following strategies to further limit the number of matrix elements to be varied according to the requirement of each case:

(i) The matrix elements were fixed when those values were known from other experiments.
(ii) In-band $E2$ matrix elements were grouped into diagonal and off-diagonal elements. They were coupled within each group, which resulted in leaving only two parameters for each band.
(iii) Interband matrix elements were grouped into three regions associated with the lower-, intermediate-, and higher-spin states—only one of which was allowed to vary at a time.
(iv) The $E1$ or $E3$ matrix elements were only allowed to vary one at a time.

Changing partners in turn to the ground-state band affected the $E2$ matrix elements within the ground-state band by no more than 0.02% during this minimization procedure. After the entire procedure, we reached a normalized $\chi^2 \sim 2.0$ as a first step.

Then we continued the minimization process further from this stage without coupling the in-band matrix elements. Instead, we took up a small group of closely related matrix elements as a free-parameter subspace one at a time and repeated the minimization by changing the subspace over the whole parameter space. Since the ^{156}Gd nucleus is well deformed, the generalized intensity relations (GIR) in the

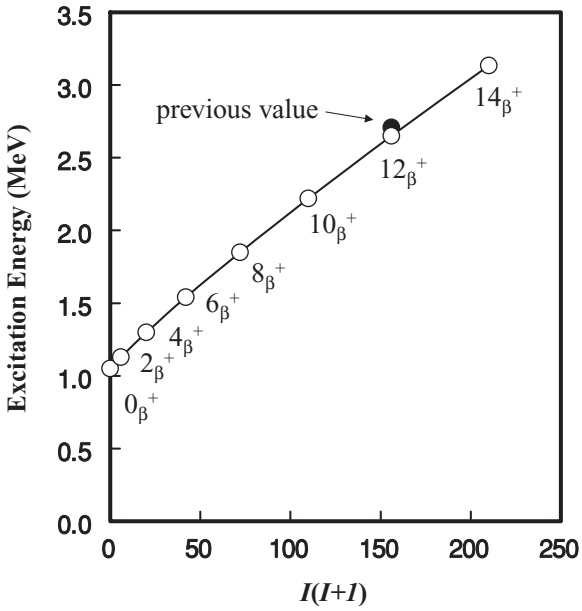

FIG. 6. Excitation energies of the states in the β band plotted against $I(I+1)$.

unified model can be used as a guiding tool to avoid unphysical matrix elements. During this process, we consulted, therefore, the GIR formulas in Ref. [4] to test the consistency of the relative phases of matrix elements. In other words, since it seemed difficult in practice to test the uniqueness of the final solution, the whole minimization process was done by referring to the unified model to circumvent local minima in the space of matrix elements. At the final stage of the minimization, we treated all the matrix elements as free parameters and reached a normalized $\chi^2 = 1.56$.

The errors in the matrix elements include cross-correlation errors, which were calculated by constructing the probability distribution in the space of fitted parameters and by requesting that the total integrated probability be equal to the chosen

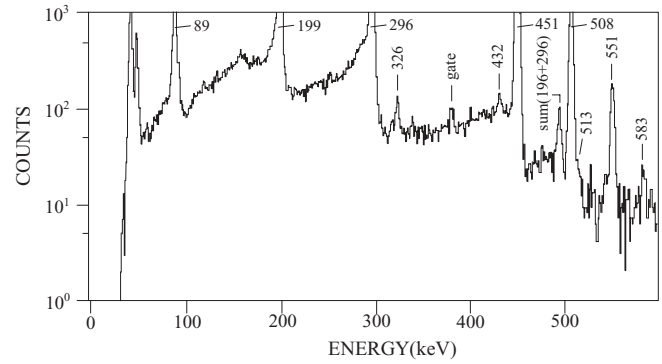

FIG. 7. γ-ray spectrum obtained by setting a gate on the 380 keV ($8^+_g \rightarrow 6^+_g$) transition. The peak at 326 keV corresponds to the $(8^+) \rightarrow 6^+$ transition in the two-quasiparticle band of $\pi_{5/2}[413] \otimes \pi_{3/2}[411]$ [2].

confidence limit (i.e., 68.3%; for details, see Ref. [15]). The overall systematic errors of 10% are added in most cases by taking into account the uncertainties in the efficiency calibration and the background subtraction for determining the γ-ray intensities.

To show the goodness of the fit, the experimental γ-ray yields are compared with the calculation as a function of scattering angle for a number of typical transitions in both the cases of the ^{32}S and ^{58}Ni beams in Figs. 9 to 12.

Since the whole minimization process has been carried out relying on the GIR as described above, it is appropriate to present the results of the fit for the intrinsic matrix elements rather than the individual matrix elements themselves. The results of the GIR fit are compared with the matrix elements obtained by the GOSIA analysis in the following figures, where the results of the previous measurements [10] are also shown for comparison.

The GIR formulas used to fit the matrix elements are taken from Shimizu and Nakatsukasa [4] and are listed below for reference:

TABLE I. Properties of γ-ray transitions from the β band to the ground-state band. Relative γ intensities are normalized to that of the $2^+_g \rightarrow 0^+_g$ transition (1000). Branching ratios are converted to B(E2) ratios assuming the $I_\beta \rightarrow I_g$ transitions are pure $E2$ transitions. Errors are given in parentheses. Theoretical values based on the Alaga rule are shown in the last two columns.

Transition	E_γ(keV)	Relative γ Intensity	$\frac{B(E2;I_\beta \rightarrow (I-2)_g)}{B(E2;I_\beta \rightarrow I_g)}$	Alaga	
$I_\beta \rightarrow I'_g$				$(K=0)$	$(K=2)$
$2_\beta \rightarrow 2_g$	1039(4)	6(5)		0.7	0.7
$4_\beta \rightarrow 4_g$	1009.5(2)	19(1)		1.1	0.34
$6_\beta \rightarrow 6_g$	956.2(5)	8(1)			
$6_\beta \rightarrow 4_g$	1252.6(3)	17(1)	0.55(8)	1.24	0.27
$8_\beta \rightarrow 8_g$	882(7)	2.0(3)			
$8_\beta \rightarrow 6_g$	1265.4(5)	6(1)	0.49(11)	1.30	0.24
$10_\beta \rightarrow 10_g$	804.3(3)	6.0(3)			
$10_\beta \rightarrow 8_g$	1255.6(6)	3.0(5)	0.054(9)	1.34	0.22
$12_\beta \rightarrow 12_g$	726.9(6)	3.0(2)			
$12_\beta \rightarrow 10_g$	1235.0(5)	3.0(3)	0.071(9)	1.37	0.21
$14_\beta \rightarrow 14_g$	659.0(4)	1.0(1)			
$14_\beta \rightarrow 12_g$	1211.0(9)	1.0(2)	0.048(11)	1.39	0.21

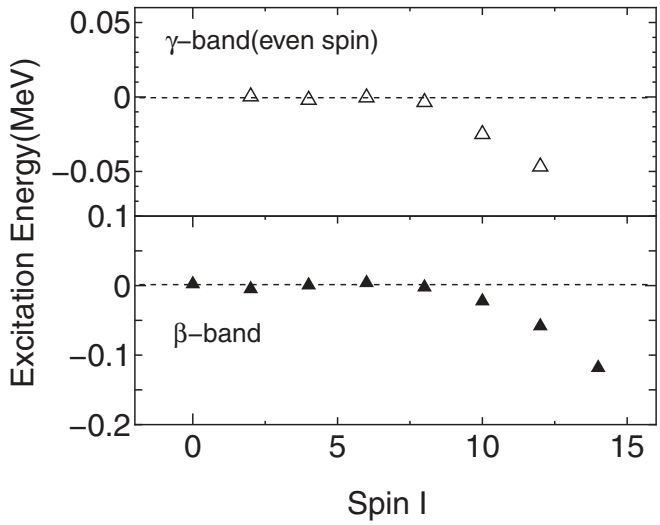

FIG. 8. Excitation energies of the γ and β bands plotted against spin I. The quadratic energy formulas emulating the behavior of lower-spin states, which are expressed as $0.0104I^2 + 0.0394I + 1.0334$ for the γ band and $0.0095I^2 + 0.0245I + 1.0472$ for the β band, are subtracted from the excitation energies.

Intraband $E2$ transitions $I - \Delta I \to I$:

$$\begin{aligned}\langle IK\|E2\|I-\Delta IK\rangle = \sqrt{2I+1}[&\langle IK20 \mid I-\Delta IK\rangle Q_0 \\ &+ (\langle IK21 \mid I-\Delta IK+1\rangle \\ &\times \sqrt{(I-\Delta I-K)(I-\Delta I+K+1)} \\ &- \langle IK2-1 \mid I-\Delta IK-1\rangle \\ &\times \sqrt{(I-\Delta I+K)(I-\Delta I-K+1)}) \\ &\times Q_1'].\end{aligned} \quad (1)$$

Here, Q_0 and Q_1' stand for the intrinsic matrix elements. However, Q_1' must vanish for $K = 0$.

Interband $E2$ transitions from the ground-state band to the $\beta(K = 0)$ and $\gamma(K = 2)$ bands $(I - \Delta I \to I)$:

$$\begin{aligned}\langle IK|E2|I-\Delta I0\rangle = \sqrt{2I+1}&\langle IK2(-K) \mid I-\Delta I0\rangle Q_t \\ &\times \big(1 + q[(I-\Delta I)(I-\Delta I+1) \\ &- I(I+1)]\big).\end{aligned} \quad (2)$$

TABLE II. Levels and matrix elements used in the GOSIA analysis. "Ground-state band" is abbreviated as "gsb" in the table.

Band	Range of Spin	Matrix Elements
gsb	$0^+ \to 22^+$	in-band $E2$
β band	$0^+ \to 14^+$	in-band $E2$
		$M1$, $E2$ from gsb
0_2^+ band	$0^+ \to 10^+$	in-band $E2$
		$M1$, $E2$ from gsb
γ band	$2^+ \to 12^+$	in-band $M1$, $E2$
	(even and odd)	$M1$, $E2$ from gsb
octupole band	$1^- \to 15^-$	in-band $E2$
$(K = 1^-)$	(only odd)	$E1$, $E3$ from gsb
octupole band	$1^- \to 3^-$	in-band $E2$
$(K = 0^-)$		$E1$, $E3$ from gsb

TABLE III. Experimental values of the lifetimes, branching ratios, mixing ratios ($E2/M1$), and the $E2$ diagonal matrix element included in the GOSIA analysis [12].

Level	Mean Lifetime (ps)
2_g^+	3188 ± 29
4_g^+	161.4 ± 2.5
6_g^+	22.8 ± 0.6
8_g^+	6.23 ± 0.33
10_g^+	2.74 ± 0.12
12_g^+	1.59 ± 0.14
2_γ^+	0.82 ± 0.03
4_β^+	2.27 ± 0.17
$2^+(0_2^+$ band)	2.22 ± 0.22
$\frac{I_i \to I_f'}{I_i \to I_f}$	Branching Ratio
$\frac{2_\beta \to 0_g}{2_\beta \to 2_g}$	0.274 ± 0.017
$\frac{2_\beta \to 4_g}{2_\beta \to 2_g}$	0.408 ± 0.019
$\frac{4_\beta \to 2_\beta}{4_\beta \to 2_g}$	0.0110 ± 0.0013
$\frac{4_\beta \to 4_g}{4_\beta \to 2_g}$	0.94 ± 0.09
$\frac{4_\beta \to 6_g}{4_\beta \to 2_g}$	0.106 ± 0.016
$\frac{2_\gamma \to 0_g}{2_\gamma \to 2_g}$	0.9620 ± 0.0077
$\frac{2_\gamma \to 4_g}{2_\gamma \to 2_g}$	0.0380 ± 0.0012
$\frac{4_\gamma \to 2_\gamma}{4_\gamma \to 4_g}$	0.0028 ± 0.0002
$\frac{4_\gamma \to 2_g}{4_\gamma \to 4_g}$	0.3800 ± 0.0055
$\frac{4_\gamma \to 6_g}{4_\gamma \to 4_g}$	0.030 ± 0.006
$\frac{2_{0_2^+} \to 0_g}{2_{0_2^+} \to 4_g}$	0.260 ± 0.011
$\frac{2_{0_2^+} \to 2_g}{2_{0_2^+} \to 4_g}$	0.710 ± 0.017
$\frac{4_{0_2^+} \to 2_{0_2^+}}{4_{0_2^+} \to 4_g}$	0.0081 ± 0.0007
$\frac{4_{0_2^+} \to 2_g}{4_{0_2^+} \to 4_g}$	0.140 ± 0.031
$\frac{4_{0_2^+} \to 6_g}{4_{0_2^+} \to 4_g}$	0.380 ± 0.038
$\frac{1_{K=1^-} \to 0_g}{1_{K=1^-} \to 2_g}$	0.971 ± 0.011
$\frac{3_{K=1^-} \to 4_g}{3_{K=1^-} \to 2_g}$	0.440 ± 0.022
$\frac{5_{K=1^-} \to 6_g}{5_{K=1^-} \to 4_g}$	0.295 ± 0.027
Transition	Mixing Ratio($E2/M1$)
$4_\gamma \to 4_g$	-4.0 ± 1.6
$3_\gamma \to 4_g$	-12.0 ± 5.0
$3_\gamma \to 2_g$	-11.8 ± 0.7
$2_\gamma \to 2_g$	-16.0 ± 5.0
$2_\beta \to 2_g$	-5.9 ± 2.8
$\langle I\|\|E2\|\|I\rangle$	$E2$ Diagonal Matrix Element
$\langle 2_g^+\|\|E2\|\|2_g^+\rangle$	-2.546 ± 0.053

Here, Q_t and q stand for the intrinsic matrix elements.

Interband $E\lambda$ ($\lambda = 1, 3$) transitions from the ground-state band to the octupole ($K = 1$) band $(I - \Delta I \to I)$:

$$\begin{aligned}\langle I1\|E\lambda\|I-\Delta I0\rangle = \sqrt{2I+1}&(\langle I1\lambda(-1) \mid I-\Delta I0\rangle Q_t \\ &\times \big(1 + q[(I-\Delta I)(I-\Delta I+1) \\ &- I(I+1)]\big) + \sqrt{(I-\Delta I)(I-\Delta I+1)} \\ &\times \langle I1\lambda0 \mid I-\Delta I1\rangle Q_t').\end{aligned} \quad (3)$$

TABLE IV. Branching ratios from the higher-spin levels of each band, either obtained from the analysis of the particle-γ-γ coincidence results or taken from the in-beam γ-ray spectroscopy [6]. These results are also included in the GOSIA analysis.

Transitions $\frac{I_i \to I'_f}{I_i \to I_f}$	Branching Ratios from particle-γ-γ	Branching Ratios from Ref. [6]
$\frac{6_\beta \to 6_g}{6_\beta \to 4_g}$	0.471 ± 0.065	
$\frac{8_\beta \to 8_g}{8_\beta \to 6_g}$	0.333 ± 0.075	
$\frac{10_\beta \to 10_g}{10_\beta \to 8_g}$	2.00 ± 0.35	
$\frac{12_\beta \to 12_g}{12_\beta \to 10_g}$	1.00 ± 0.12	
$\frac{14_\beta \to 14_g}{14_\beta \to 12_g}$	1.00 ± 0.22	
$\frac{6_\gamma \to 6_g}{6_\gamma \to 4_g}$	2.32 ± 0.18	
$\frac{6_\gamma \to 4_\gamma}{6_\gamma \to 4_g}$	0.161 ± 0.014	
$\frac{8_\gamma \to 6_\gamma}{8_\gamma \to 8_g}$	0.200 ± 0.027	
$\frac{8_\gamma \to 6_\gamma}{8_\gamma \to 8_g}$	0.400 ± 0.032	
$\frac{9_\gamma \to 7_\gamma}{9_\gamma \to 8_g}$		0.188 ± 0.033
$\frac{10_\gamma \to 8_g}{10_\gamma \to 10_g}$	0.88 ± 0.13	
$\frac{10_\gamma \to 8_\gamma}{10_\gamma \to 10_g}$	1.000 ± 0.063	
$\frac{11_\gamma \to 9_\gamma}{11_\gamma \to 10_g}$		2.50 ± 0.40
$\frac{12_\gamma \to 10_\gamma}{12_\gamma \to 12_g}$	1.00 ± 0.28	
$\frac{9_{K=1^-} \to 10_g}{9_{K=1^-} \to 8_g}$		0.37 ± 0.16
$\frac{11_{K=1^-} \to 9_{K=1^-}}{11_{K=1^-} \to 10_g}$		0.138 ± 0.070
$\frac{13_{K=1^-} \to 11_{K=1^-}}{13_{K=1^-} \to 12_g}$		0.160 ± 0.042
$\frac{15_{K=1^-} \to 13_{K=1^-}}{15_{K=1^-} \to 14_g}$		0.273 ± 0.052

Here, Q_t, q, and Q'_t stand for the intrinsic matrix elements. However, Q'_t must vanish for $E1$ transitions.

III. INTRINSIC MATRIX ELEMENTS FOR THE POSITIVE-PARITY BANDS

The intrinsic matrix elements are extracted for the $E2$ transitions within the positive-parity bands by adjusting the parameters in the GIR formula (1) to reproduce the matrix elements. The Q_0 value for the ground-state band is obtained as $Q_0 = 2.22 \pm 0.04$ eb and the results of the fit are compared with the matrix elements reached by the GOSIA analysis in the upper part of Fig. 13. The spin dependence of the in-band $E2$ matrix elements for the ground-state band is well reproduced by the GIR calculation with a single parameter Q_0. That means ^{156}Gd is a good rotor as far as the ground-state band is concerned.

For the β band, the structural change is suggested between the 8^+ and 10^+ states in Sec. II A. Moreover, it is inferred from the reduction of $B(E2)$ ratios that this might be caused by the change of the K value of the band. Therefore the intrinsic matrix elements are extracted separately for the states of $I \leqslant 8$ and $I \geqslant 10$ with and without, respectively, the change of K value from 0 to 2 between 8^+ and 10^+. The results of the fit are shown in the lower part of Fig. 13 where those with and without the change of K value are drawn with the dotted and

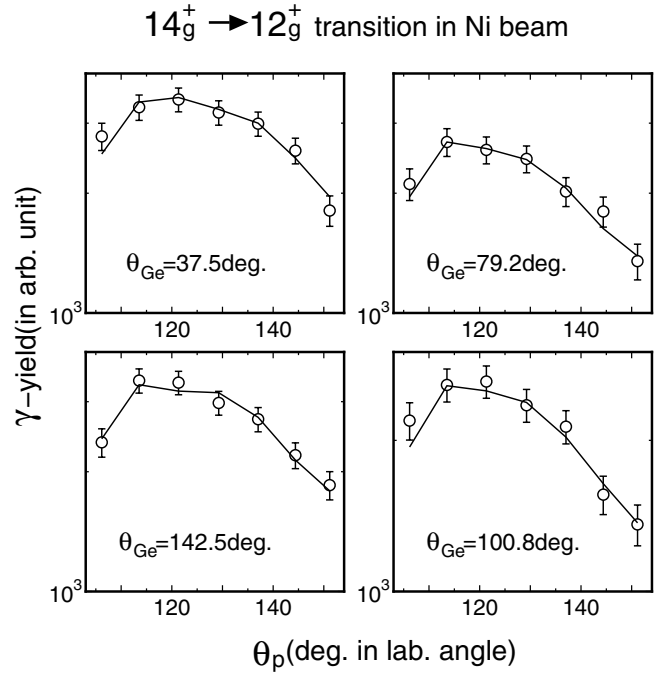

FIG. 9. Experimental γ-ray yields compared with calculation as a function of scattering angle for the 551 keV ($14_g \to 12_g$) transition in the case of the ^{58}Ni beam.

solid lines, respectively. The values obtained are as follows:

$I \leqslant 8(K = 0)$, $Q_0 = 2.7 \pm 0.2$ eb,
$I \geqslant 10(K = 0)$, $Q_0 = 1.8 \pm 0.2$ eb,
$I \geqslant 10(K = 2)$, $Q_0 = 0.8 \pm 0.3$ eb, $Q'_1 = 0.18 \pm 0.04$ eb.

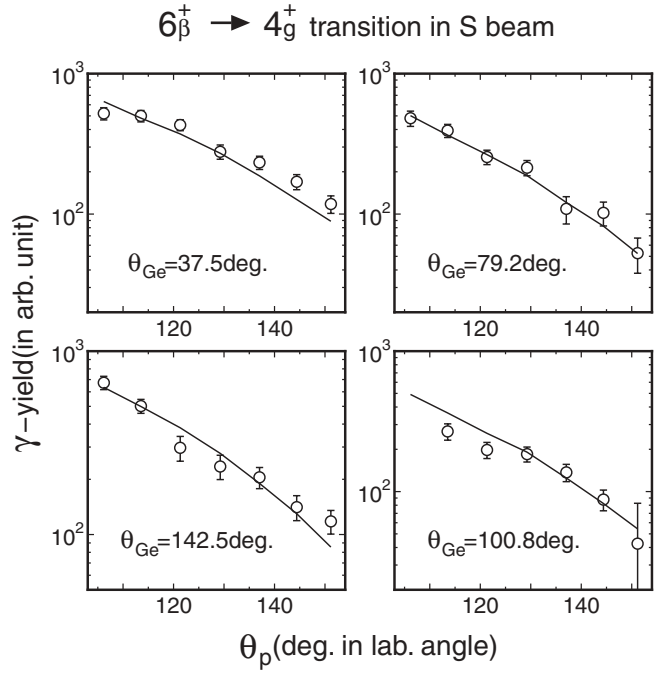

FIG. 10. Experimental γ-ray yields compared with calculation as a function of scattering angle for the 1253 keV ($6_\beta \to 4_g$) transition in the case of the ^{32}S beam.

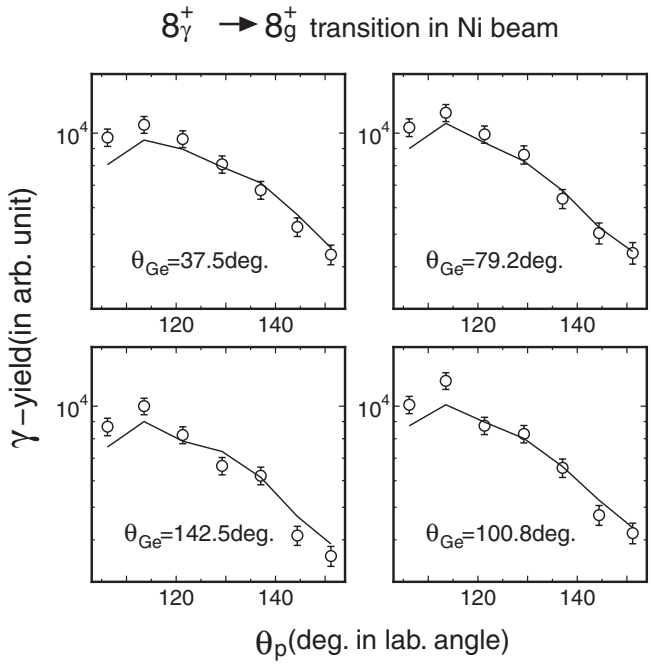

FIG. 11. Experimental γ-ray yields compared with calculation as a function of scattering angle for the 1045 keV ($8_\gamma \rightarrow 8_g$) transition in the case of the ^{58}Ni beam.

While Q_0 of the β band for the lower-spin states is appreciably larger than that of the ground-state band, the value for the higher-spin states is quite small in either case. It turns out that, assuming the higher-spin states of the β band to be of $K = 2$, improves the fit as shown in Fig. 13. This constitutes evidence

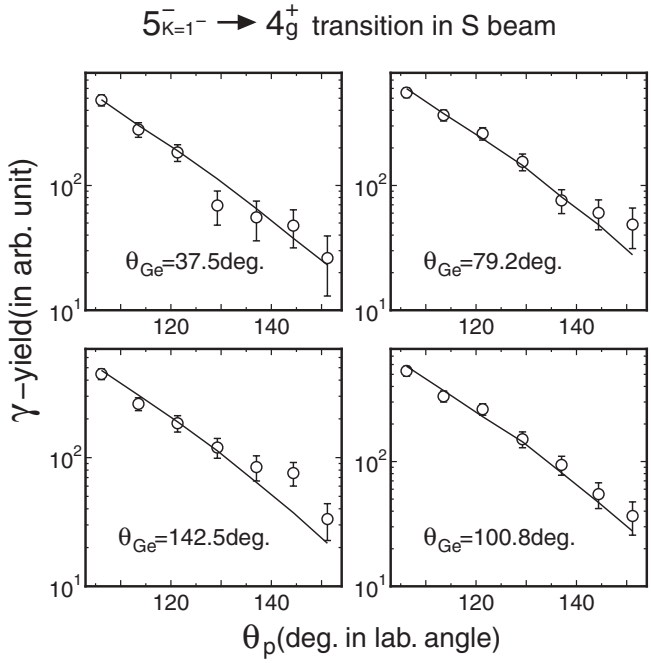

FIG. 12. Experimental γ-ray yields compared with calculation as a function of scattering angle for the 1118 keV ($5^-_{K=1^-} \rightarrow 4_g$) transition in the case of the ^{32}S beam.

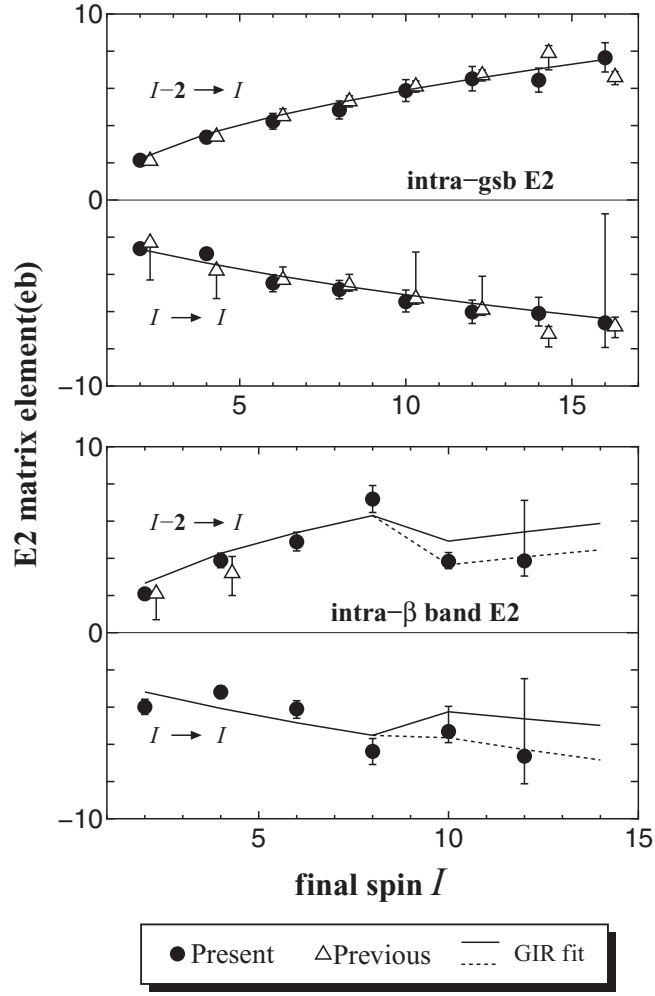

FIG. 13. $E2$ matrix elements reached by GOSIA analysis compared with the results of the GIR fit for the transitions within the ground-state band and the β band. The values from Ref. [10] are also plotted for comparison. For the difference between the solid and dotted lines, see the text.

supporting the structural change in the β band suggested in Sec. II A. However, since the value of Q'_1 is unexpectedly large, it would be cautious not to take this value literally.

The similar structural change is also suggested between the 8^+ and 10^+ states for the γ band from the spin dependence of the excitation energy shown in Fig. 8. Therefore, the same strategy is adopted to obtain the intrinsic matrix elements for the γ band. However, since the $K = 0$ band consists of only even-spin states, it is necessary to fit separately to the matrix elements associated with odd- and even-spin states. Consequently, while the odd-spin states are assumed to be of $K = 2$ through the whole spin region, the even-spin states are assumed to change their K values from 2 to 0 between the 8^+ and 10^+ states. The results of the fit are shown for the matrix elements associated with the odd- and even-spin states in Figs. 14 and 15, respectively. While the solid line in Fig. 15 represents the results of the fit to the lower-spin states, the dotted line shows the results of the fit with the change of K

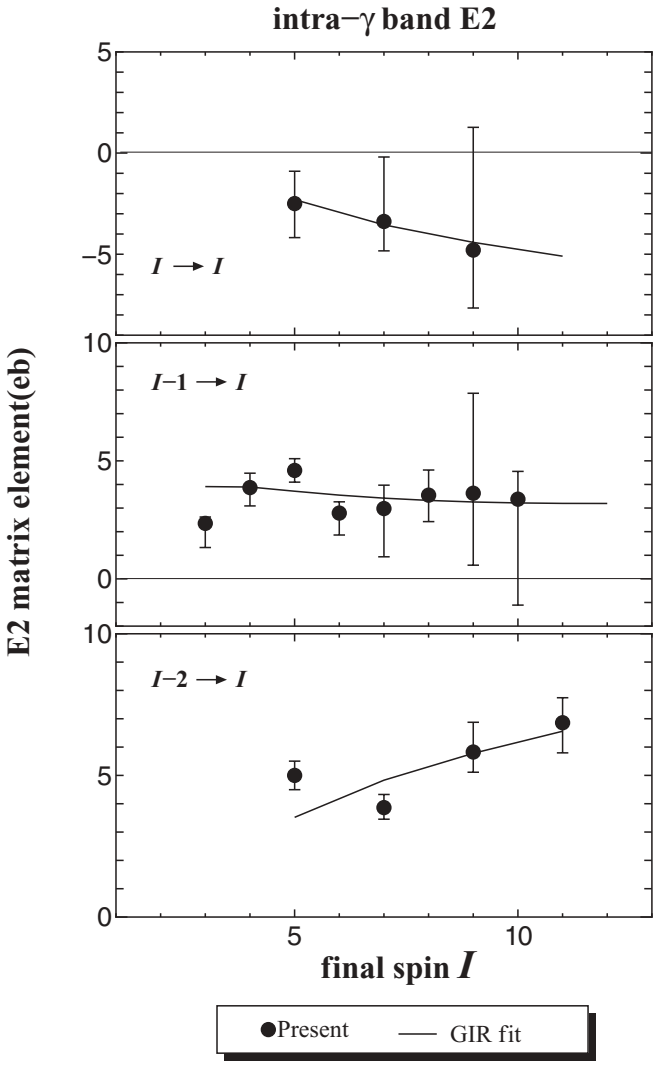

FIG. 14. $E2$ matrix elements reached by GOSIA analysis compared with the results of the GIR fit for the transitions associated with the odd-spin members within the γ band.

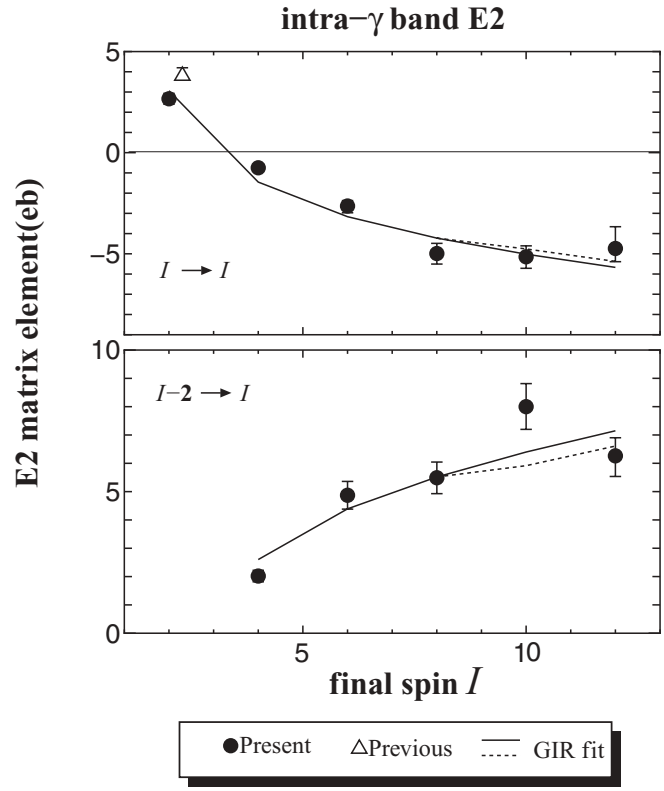

FIG. 15. $E2$ matrix elements reached by GOSIA analysis compared with the results of the GIR fit for the transitions associated with the even-spin members within the γ band. The values from Ref. [10] are also plotted for comparison. For the difference between the solid and dotted lines, see the text.

values in the higher-spin states. The obtained values are as follows:

Transitions associated with the odd-spin states:

$K = 2, \quad Q_0 = 2.5 \pm 0.1$ eb, $Q_1' = -0.014 \pm 0.010$ eb.

Transitions associated with the even-spin states:

$I \leqslant 8(K = 2), \quad Q_0 = 2.5 \pm 0.4$ eb,

$Q_1' = -0.009 \pm 0.052$ eb,

$I \geqslant 10(K = 0), \quad Q_0 = 2.3 \pm 0.2$ eb.

The Q_0 of the γ band for the lower-spin states lies between those of the ground-state band and the β band. It is seen that the Q_0 value for the higher-spin states is slightly reduced. This can be considered as evidence for the structural change in the γ band suggested in Sec. II A, although the values for the lower- and higher-spin states overlap each other within errors.

The intrinsic matrix elements are extracted for the $E2$ transitions from the ground-state band to the β and γ bands by adjusting the parameters in the GIR formula (2) to reproduce the matrix elements. The fitting is made separately for the states of $I \leqslant 8$ and $I \geqslant 10$ in both the β and γ bands with and without the change of K values, respectively. The results of the fit with and without the change of K values are shown for the β band with the dotted and solid lines, respectively, in Fig. 16. The obtained values are as follows:

$I \leqslant 8(K = 0), \quad Q_t = 0.21 \pm 0.06$ eb,
$q = -0.026 \pm 0.013$,

$I \geqslant 10(K = 0), \quad Q_t = 0.006 \pm 0.062$ eb,
$q = 0.3 \pm 2.9$,

$I \geqslant 10(K = 2), \quad Q_t = -0.005 \pm 0.082$ eb,
$q = 0.4 \pm 6.6$.

The values for the lower-spin states can be compared with the calculations by Shimizu and Nakatsukasa [4] in which the values of $Q_t = 0.171$ eb and $q = 0.042$ are tabulated. While Q_t is consistent, the sign of q does not match. Although the intrinsic matrix elements are deduced reliably for the lower-spin states, the obtained values for the higher-spin states are plagued with serious errors because of the insufficient data points. Therefore it is fair to say that it cannot be concluded from these results whether the change of K values really happens in the β band or not. However, it can be recognized that the Q_t values drop abruptly for the higher-spin states

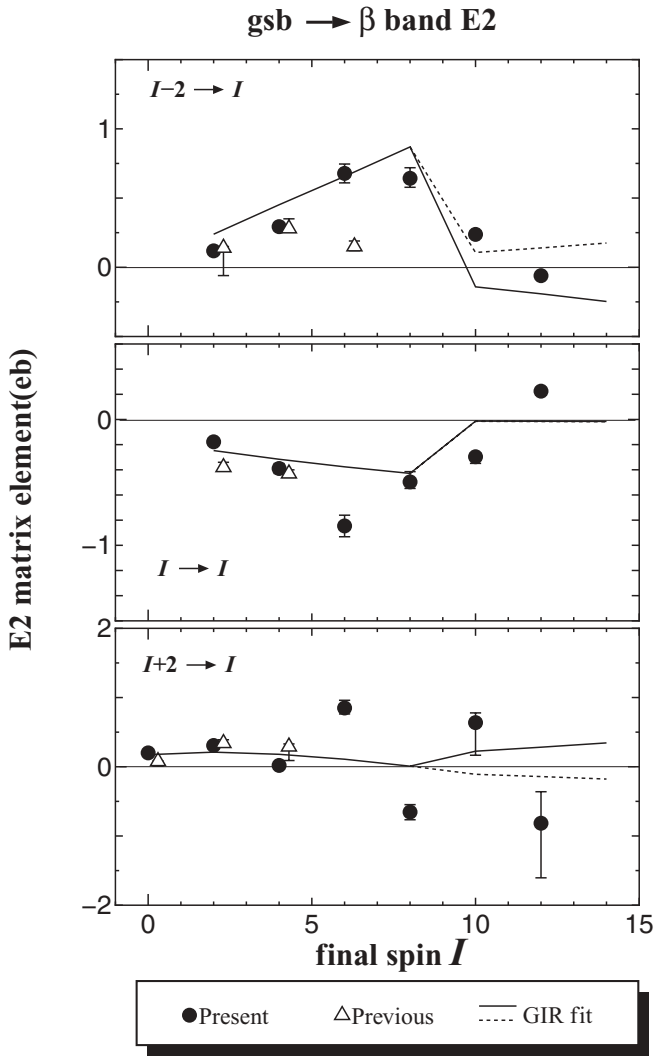

FIG. 16. $E2$ matrix elements reached by GOSIA analysis compared with the results of the GIR fit for the interband transitions from the ground-state band to the β band. The values from Ref. [10] are also plotted for comparison. "Ground-state band" is abbreviated as "gsb" in the figure. For the difference between the solid and dotted lines, see the text. For the transitions from I to I, the differences between the solid and dotted lines are invisibly small in this figure.

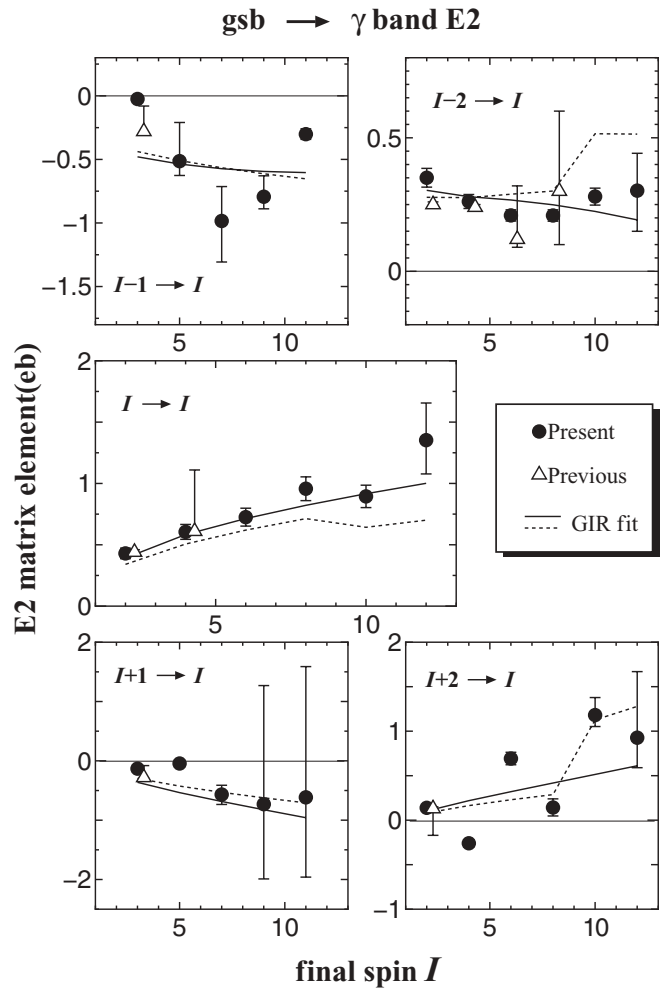

FIG. 17. $E2$ matrix elements reached by GOSIA analysis compared with the results of the GIR fit for the interband transitions from the ground-state band to the γ band. The values from Ref. [10] are also plotted for comparison. "Ground-state band" is abbreviated as "gsb" in the figure. For the difference between the solid and dotted lines, see the text.

even if we allow for the large errors. Additionally, it is important to note that the oscillating pattern is observed for $\langle I_\beta \| E2 \| (I+2)_g \rangle$ in the higher-spin region (see bottom part of Fig. 16).

The similar approach is taken to obtain the intrinsic matrix elements for the $E2$ transitions from the ground-state band to the γ band. The results of the fit are shown in Fig. 17. First, a fit is made separately for the states of $I \leqslant 8$ and $I \geqslant 10$ with the change of K values from 2 to 0 (see dotted line in the figure). Second, another fit is made assuming that the γ is a single $K = 2$ band through the whole spin region (see solid line in the figure). The obtained results are as follows:

with the change of K values:

$I \leqslant 8(K = 2), \quad Q_t = 0.29 \pm 0.04$ eb,
$q = 0.005 \pm 0.008$,

$I \geqslant 10(K = 0), \quad Q_t = 0.28 \pm 0.04$ eb,
$q = 0.008 \pm 0.004$;

a single $K = 2$ band:

$Q_t = 0.33 \pm 0.03$ eb, $\quad q = 0.013 \pm 0.005$.

The values for the lower-spin states can be compared with the calculations by Shimizu and Nakatsukasa [4] in which the values of $Q_t = 0.391$ eb and $q = 0.024$ are tabulated. The present values are slightly smaller for both Q_t and q. The intrinsic matrix elements are extracted for the higher-spin states in the γ band more reliably than those for the β band. Although the qualitative behavior seen in the higher-spin region in Fig. 17 may seem to prefer the change of the K values, it is fair to say that these two results have an equal quality of fit. Additionally, it should be noted that the oscillating pattern is observed for $\langle I_\gamma \| E2 \| (I+2)_g \rangle$. This is quite similar to the one observed in the β band and the phase of oscillation also coincides with each other's. We called attention in the introduction to the fact that

the level order of the 0^+_β state and the 2^+_γ state is reversed between ^{156}Gd and ^{158}Gd. A strong interaction, therefore, can be expected between the β and γ bands in ^{156}Gd. In fact, Bäcklin *et al.* carried out a four-band-mixing calculation involving the ground-state band, the β band, the $K = 0^+_2$ band, and the γ band, and obtained a quite good agreement between experiment and calculation for the $E2$ transition probabilities associated with lower-spin ($I \leqslant 4$) states [16].

As mentioned in the introduction, it is important to characterize the nature of the $K = 0^+_2$ band. The Q_0 value of 1.45 ± 0.13 eb is obtained for the $E2$ transitions within this band. The smaller Q_0 value suggests the smaller deformation for the $K = 0^+_2$ band.

IV. INTRINSIC MATRIX ELEMENTS FOR THE NEGATIVE-PARITY BANDS

Although we tried to observe a complete set of the octupole bands, we could not observe the decaying γ rays from other than the $K = 0^-$ and $K = 1^-$ bands. The intrinsic matrix elements are extracted for the $E2$ transitions within the $K = 1^-$ band by adjusting the parameters in the GIR formula (1) to reproduce the matrix elements. The Q_0 and Q'_1 values for the $K = 1^-$ band are obtained as $Q_0 = 2.49 \pm 0.14$ eb and $Q'_1 = 0.22 \pm 0.16$ eb. The results of the fit are compared with the matrix elements reached by the GOSIA analysis in Fig. 18. The Q_0 value for the $K = 1^-$ band turns out to be slightly larger than that for the ground-state band and comparable to that for the γ band.

The intrinsic matrix elements are extracted for the $E1$ and $E3$ transitions from the ground-state band to the $K = 1^-$ octupole band by adjusting the parameters in the GIR formula (3) to reproduce the matrix elements. It is well known that $E1$ matrix elements are quite sensitive to the microscopic

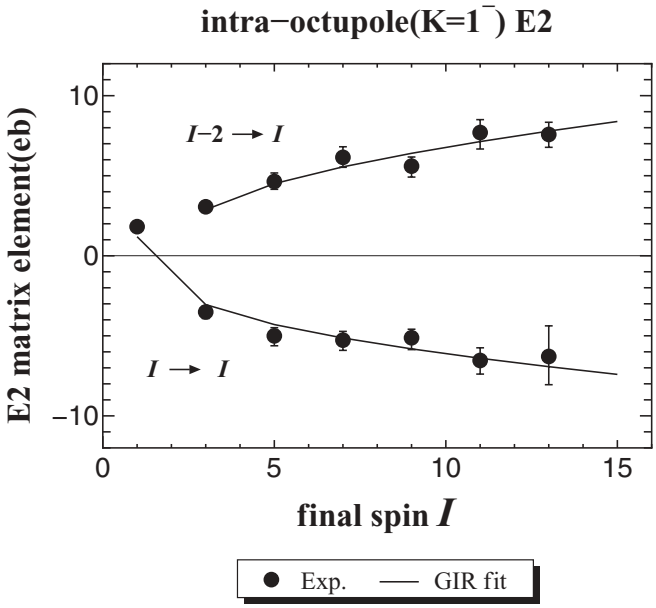

FIG. 18. $E2$ matrix elements reached by GOSIA analysis compared with the results of the GIR fit for the transitions within the $K = 1^-$ band.

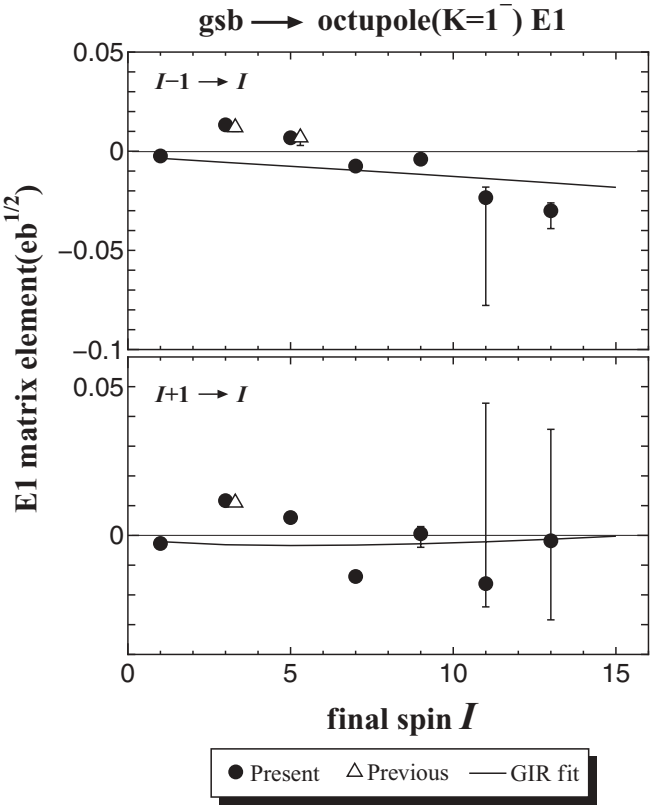

FIG. 19. $E1$ matrix elements reached by GOSIA analysis compared with the results of the GIR fit for interband transitions from the ground-state band to the $K = 1^-$ octupole band. The values from Ref. [10] are also plotted for comparison. "Ground-state band" is abbreviated as "gsb" in the figure.

structures of states [17]. Accordingly, it should be kept in mind that the values obtained can only respond the average behavior. The results of the fit are shown in Fig. 19 and the values obtained are as follows:

$$Q_t = -0.0034 \pm 0.0016 \text{ eb}^{1/2}, \quad q = -0.03 \pm 0.03.$$

The results of the fit are shown in Fig. 20 for the $E3$ transitions from the ground-state band to the $K = 1^-$ octupole band. The values obtained are as follows:

$$Q_t = 0.44 \pm 0.08 \text{ eb}^{3/2}, \quad q = 0.004 \pm 0.005,$$
$$Q'_t = 0.009 \pm 0.010 \text{ eb}^{3/2}.$$

These values are quite different from the calculations by Shimizu and Nakatsukasa [4] in which the values of $Q_t = 0.111$ eb$^{3/2}$, $q = -0.227$ and $Q'_t = 0.065$ eb$^{3/2}$ are tabulated. Additionally, it should be noted that a strong enhancement has been observed for the $E3$ transitions from the ground-state band to the $K = 1^-$ octupole band. This enhancement corresponds to the $B(E3 : 3^- \rightarrow 0^+)$ value as large as 20 Weisskopf units. Such an enhancement was not observed for the $K = 0^-$ octupole band. There is another interesting point one can easily recognize in Fig. 20: The values for the $\Delta I = -3$ and 3 transitions to the 9^- state are strongly reduced.

We could not observe the decaying γ rays from the $K = 2^-$ octupole band such as 1564 keV ($3^-_{K=2} \rightarrow 4^+_g$) and 1763 keV ($3^-_{K=2} \rightarrow 2^+_g$), while we could barely observe the decaying γ

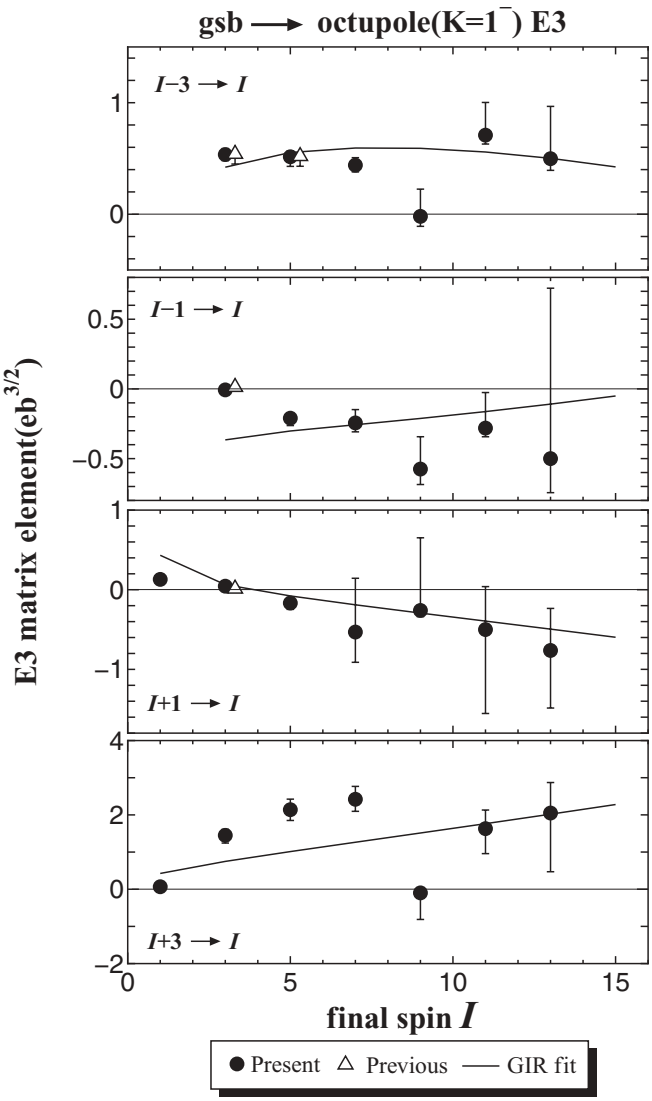

FIG. 20. $E3$ matrix elements reached by GOSIA analysis compared with the results of the GIR fit for interband transitions from the ground-state band to the $K = 1^-$ octupole band. The values from Ref. [10] are also plotted for comparison. "Ground-state band" is abbreviated as "gsb" in the figure.

rays from the $K = 0^-$ octupole band such as 988 keV ($3^-_{K=0} \rightarrow 4^+_g$) and 1187 keV ($3^-_{K=0} \rightarrow 2^+_g$). We can set, therefore, the upper bound of $\langle 3^-_{K=2^-}||E3||0_{g^+}\rangle$ to be of the order of 0.01 $eb^{3/2}$ considering the value of $\langle 3^-_{K=0^-}||E3||0_{g^+}\rangle \sim 0.02\ eb^{3/2}$, which is deduced from the present experiment, and the relative efficiencies for the corresponding γ rays.

V. CONCLUSIONS

We have made multiple Coulomb-excitation experiments of ^{156}Gd with a 118 MeV ^{32}S beam and a 225 MeV ^{58}Ni beam. The following results have been obtained from the analysis of the E_γ-E_γ matrix. The ground-state band and the γ band were observed to the 18^+ and 12^+ states, respectively. The 12^+_γ state is placed at 2957 keV in the present experiment, while our previous in-beam γ-ray spectroscopy [6] suggested the existence of the 12^+ state at 2922 keV as a member of the positive-parity side-band. These facts indicate that the band crossing occurs at the 12^+ state in the γ band. We extend the β band to the 14^+ state and the excitation energy of the 12^+ state we observed is a little lower than that of the previously assigned 12^+ state. The present energy value has turned out to fit in with the smooth behavior of the band. The reduction of $B(E2)$ ratios shown in Table I suggests that the β band might change its character around the 10^+ state. The change of K values in the β and γ bands is discussed as a possible cause for this structural change.

The intrinsic matrix elements are extracted for both in-band transitions and interband transitions from the ground-state band by adjusting the parameters in the GIR formulas to reproduce the matrix elements obtained through the least-squares search code GOSIA based on the particle-γ angular correlation. It turns out that the magnitude of Q_0 increases in the order of the ground-state band, the γ band, and the β band. The spin dependence of the in-band $E2$ matrix elements is reasonably described for the ground-state band, the β band, and the γ band. The behavior of the $E2$ matrix elements in the higher-spin region in the β and γ bands is consistent with the interpretation that these two bands change their characters in the higher-spin region. The oscillating patterns are observed for the interband $E2$ matrix elements in the β and γ bands.

We could not observe the decaying γ rays from the octupole bands other than $K = 0^-$ and $K = 1^-$. As for the $K = 1^-$ octupole band, the intrinsic matrix elements are extracted for the $E2$ transitions within the band and the $E1$ and $E3$ transitions from the ground-state band. The value of Q_0 for the $K = 1^-$ octupole band turns out to be comparable to that for the γ band. For the $E3$ matrix elements from the ground-state band to the $K = 1^-$ octupole band, a strong enhancement as large as around 20 Weisskopf units of $B(E3 : 3^- \rightarrow 0^+)$ is observed.

ACKNOWLEDGMENTS

We would like to thank Dr. B. Herskind, Dr. G. Sletten, Mr. J. Westergaard, and the members of Tandem Accelerator Laboratory, Niels Bohr Institute, for their kind support. We also would like to express our sincere gratitude to Professor Claes Fahlander for letting us refer to the Ph.D. thesis of one of his group members, Dr. B. Varnestig. A part of this research is supported by Monbusho International Scientific Research Program (Joint Research No. 01044037).

[1] Y. Yoshizawa, B. Elbek, B. Herskind, and M. C. Olesen, Nucl. Phys. **73**, 273 (1965).

[2] R. B. Firestone and V. S. Shirley, *Table of Isotopes*, 8th ed. (John Wiley & Sons Inc., New York, 1996).

[3] Å. Bohr and B. Mottelson, *Nuclear Structure*, Vol. 4, Chap. 4 (Benjamin, New York, 1975).
[4] Y. R. Shimizu and T. Nakatsukasa, Nucl. Phys. A **611**, 22 (1996).
[5] G. Sletten, in *Proceedings of the International Seminar on the Frontier of Nuclear Spectroscopy*, edited by Y. Yoshizawa *et al.* (World Scientific, Singapore, 1993), p. 129.
[6] M. Sugawara *et al.*, Nucl. Phys. A **686**, 29 (2001).
[7] J. Konijn, F. W. N. D. Boer, A. V. Poelgeest, W. H. A. Hesselink, M. J. A. D. Voigt, and H. Verheul, Nucl. Phys. A **352**, 191 (1981).
[8] F. K. McGowan and W. T. Milner, Phys. Rev. C **23**, 1926 (1981).
[9] M. Sugawara, H. Kusakari, T. Morikawa, H. Inoue, Y. Yoshizawa, A. Virtanen, M. Piiparinen, and T. Horiguchi, Nucl. Phys. A **557**, 653c (1993).
[10] B. Varnestig, Ph.D. thesis (unpublished), University of Uppsala (1987).
[11] B. Herskind, Nucl. Phys. A **447**, 395c (1985).
[12] C. W. Reich, Nucl. Data Sheets **99**, 753 (2003).
[13] D. Radford, Nucl. Instrum. Methods Phys. Res., Sect. A **361**, 297 (1995).
[14] T. Czosnyka, D. Cline, and C. Y. Wu, Bull. Am. Phys. Soc. **28**, 745 (1983).
[15] T. Czosnyka, D. Cline, L. Hasselgren, and C. Y. Wu, Nucl. Phys. A **458**, 123 (1986).
[16] A. Bäcklin *et al.*, Nucl. Phys. A **380**, 189 (1982).
[17] I. Hamamoto, Nucl. Phys. A **557**, 515c (1993).